JOURNAL OF MATERIALS SCIENCE 28 (1993) 3665–3669

Effect of ceramic reinforcement on the ageing behaviour of an aluminium alloy

M. J. HADIANFARD, YIU-WING MAI, J. C. HEALY
Centre for Advanced Materials Technology, Department of Mechanical Engineering, University of Sydney, Sydney, New South Wales 2006, Australia

The effect of a 20 vol % alumina microsphere particulate on the age-hardening characteristics of a 6061 Al matrix composite was investigated – based on microhardness, electrical resistivity and X-ray mapping – and the composite is compared to the unreinforced 6061 Al alloy. It is shown that this ceramic reinforcement can affect the age-hardening behaviour of the matrix alloy by significantly accelerating the kinetics of precipitation. This acceleration is related to a decrease in nucleation time and to an increase in the precipitate-growth rate. The relative amounts of age-hardened precipitates are also observed to be affected by reinforcement addition.

1. Introduction

The presence of ceramic reinforcement can considerably influence the age hardening of aluminium alloys [1]. Nieh and Karalk have shown that reinforcement of B_4C particles in AA6061 reduced the peak ageing time by a factor of three [2]. Fiorini also observed that in Al_2O_3/Al–Mg–Si and Al–Cu metal matrix composites (MMCs) an alumina content of approximately three per cent was enough to inhibit GP-zone formation [3, 4] (see Section 4 for discussion of GP zones). Schueller and Wawner found that the time required for solution formation of 15 vol % SiC-reinforced aluminium alloy in solution heat treatment was much shorter than for the matrix alloy [5]. Friend measured the resistivity and hardness of 6061 aluminium reinforced with δ-alumina fibres and found that the alumina fibres suppressed GP-zone formation, which inhibited natural ageing and considerably reduced the peak hardening during artificial ageing [6]. Differential scanning calorimetry (DSC) studies have established that the addition of SiC to an aluminium alloy does not alter the precipitation sequence of the matrix, only that the kinetics are different [7, 8]. The more rapid ageing in MMCs has been attributed to a higher diffusion rate resulting from a higher dislocation density [9]. These high-dislocation zones are formed because of the notably different thermal-expansion coefficients between the matrix and the ceramic reinforcement [10, 11]. Both the dislocation density and its distribution affect the overall rate of accelerated ageing [2].

Thus the presence of the reinforcing phase influences the matrix microstructure, which in turn can significantly affect the mechanical properties of MMCs. An investigation of the effect of ceramic reinforcement in matrix precipitation is important since it helps the ageing behaviour of MMCs to be understood. This study used a range of experimental techniques to broaden this understanding by investigating the ageing behaviour of 6061 reinforced with 20 vol % alumina microspheres and comparing the results obtained to those of the unreinforced 6061 alloy.

2. Experimental details

2.1. Material

The composite material investigated was Comral-85, a 6061 aluminium alloy containing 20 vol % spherical alumina particles. The material was produced by liquid metallurgy at the Comalco Research Centre, Thomastown, Victoria, and extruded to plates of 12.5 mm thickness and 75 mm width. The alumina microspheres had diameters between 3 and 50 μm with the majority between 10 and 30 μm, with an average diameter of 17.5 μm. The unreinforced-matrix 6061 aluminium produced by the same route was also investigated. Both materials were subjected to the following heat treatments: (a) solution heat treatment at 530 °C for 1.5 h, (b) cold-water quenching at room temperature, and (c) age hardening at 175 °C for a time varying from 0 to 68 h.

2.2. Metallography

Three ageing conditions were investigated; under-aged (UA), peak-aged (T6) and over-aged (OA). Prior to optical examination, all specimens were polished and etched with hydrofluoric acid (HF). A large number of secondary particles, whose distribution and size were non-uniform, were observed for all heat treatments in the reinforced material. EDAX analysis of these particles showed that they consisted of Fe, Al, Si and Cr (Fig. 1). Metallographic examination of the unreinforced alloy showed the presence of the same inclusions, varying between 0.5 and 2 μm in size.

0022–2461

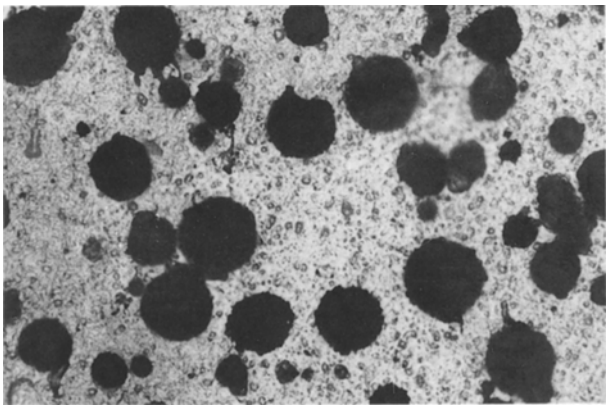

Figure 1 The microstructure of the MMC.

2.3. Microhardness test

The microhardness of the unreinforced alloy and MMC was measured on polished surfaces of specimens, which were aged artificially at 175 °C for between 0 and 68 h. The measurements were carried out using a Vickers microhardness-testing machine with an applied load of 0.1 kg and a loading time of 15 s. For each specimen ten measurements within the matrix, away from any particles, were obtained.

2.4. Resistivity test

Resistivity measurements were carried out on specimens that were 130 mm long, 12 mm thick and 32 mm wide according to ASTM Standard B 139, using a four-probe direct-current technique. Both the unreinforced alloy and the MMC were solution treated, quenched and put in a furnace for up to 20 h at 175 $\pm$ 2 °C. A direct current of 2.5 A was passed through two outer probes and the voltage drop between the inner probes was measured. The resistivity, Γ, was calculated by

$$\Gamma = RA/L \quad (1)$$

where R, A and L are the resistance of specimen, cross-sectional area and distance between inner probes, respectively.

2.5. X-ray mapping

The distributions of Al, Mg, Si, Fe, Ti, Mn and Cr elements were determined by X-ray maps, from energy dispersive spectroscopy (EDX) and wavelength dispersive spectroscopy (WDS), on the polished surfaces of the UA, T6 and OA specimens of both the unreinforced and reinforced materials. Microprobe and scanning electron microscopy (SEM) were used for the mapping. The ageing condition of the MMC had a significant effect on the distribution of elements.

3. Results

Results from microhardness measurements are shown in Fig. 2. The two curves for both materials show the same general features, but there are clear differences between the two. The time to reach maximum hardness is less in the MMC than in the unreinforced alloy (8 h compared to 11 h), and H_V for the MMC in both the solution heat treated and T6 conditions is higher than that of the unreinforced alloy. However, the composite loses its hardness faster than the unreinforced alloy in the OA condition.

Fig. 3 shows the results of the resistivity tests. The general shape of the resistivity curves for the reinforced alloy and unreinforced matrix is again similar. The resistivity in the MMC reached its maximum resistivity after 1.5 h, whilst the unreinforced alloy reached its maximum resistivity after 5.5 h. The maximum change in resistivity was also different for each material, being 0.68×10^{-9} Ω m for the composite and 2.4×10^{-9} Ω m for the unreinforced alloy. Figs 4–6 show Mg distribution as a function of ageing time at 175 °C for the MMC and the unreinforced 6061 aluminium. Whilst the distribution of Mg in the unreinforced alloy for all under aged conditions was nearly homogeneous, segregation of Mg was seen in MMCs aged for more than 1.5 h. The segregation of Mg

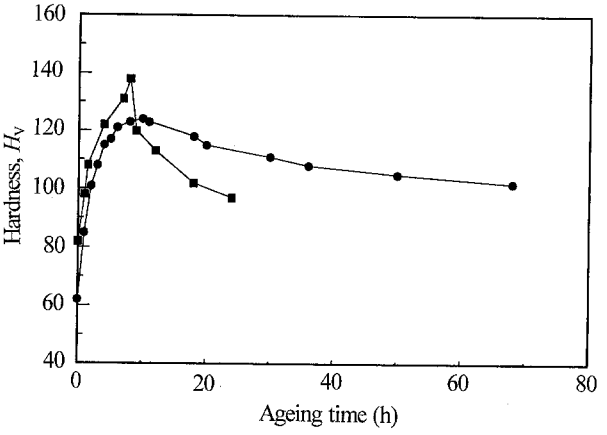

Figure 2 Vickers hardness, H_V, measurements versus ageing time: (■) 6061 Al MMC, and (●) 6061 Al alloy.

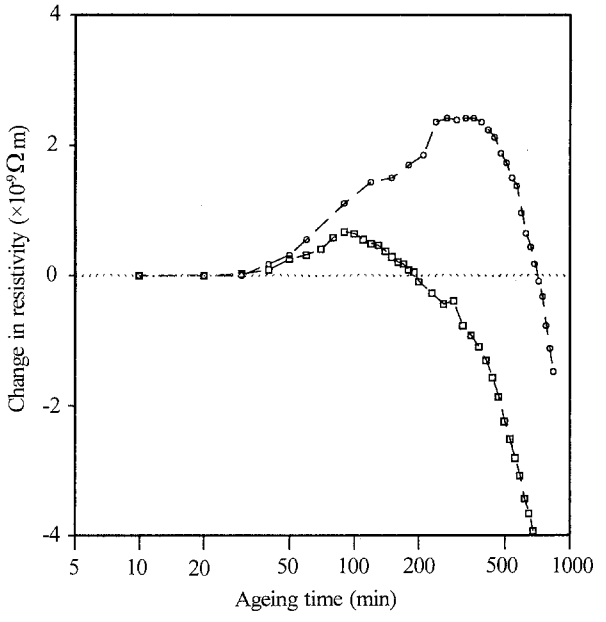

Figure 3 Change in resistivity with ageing time at 175 °C for: (○) 6061 Al alloy, and (□) 6061 Al MMC.

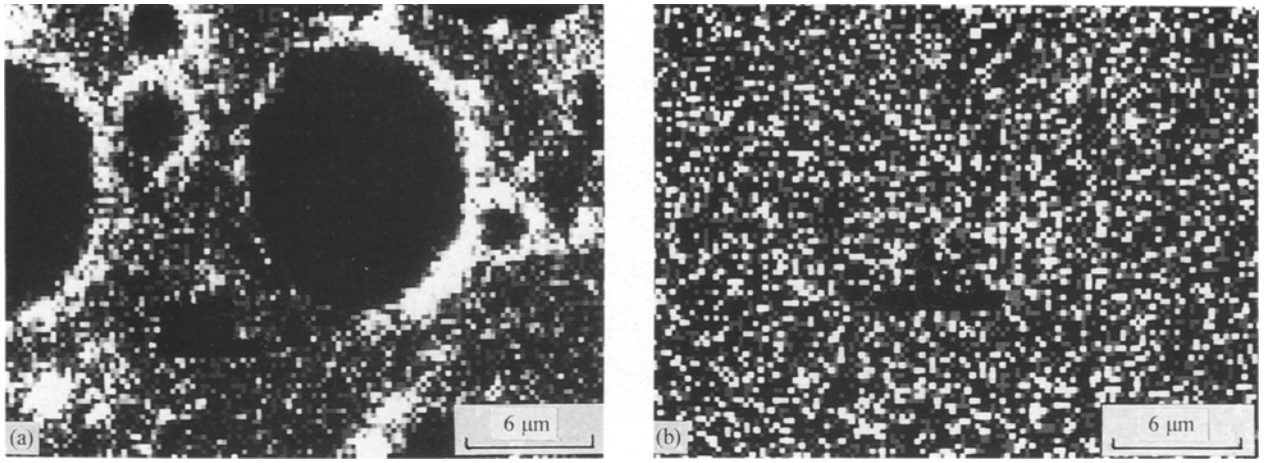

Figure 4 The X-ray maps (MgK_α) for specimens after 2 h ageing at 175 °C: (a) MMC, and (b) unreinforced alloy.

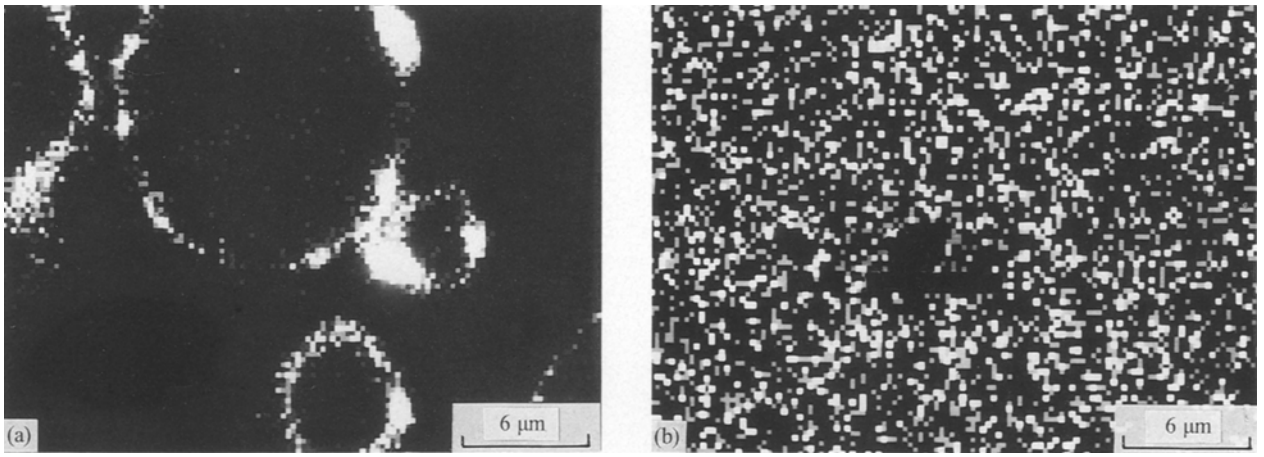

Figure 5 The X-ray maps (MgK_α) for specimens at the T6 condition: (a) MMC (after 8 h at 175 °C), and (b) unreinforced alloy (after 11 h at 175 °C).

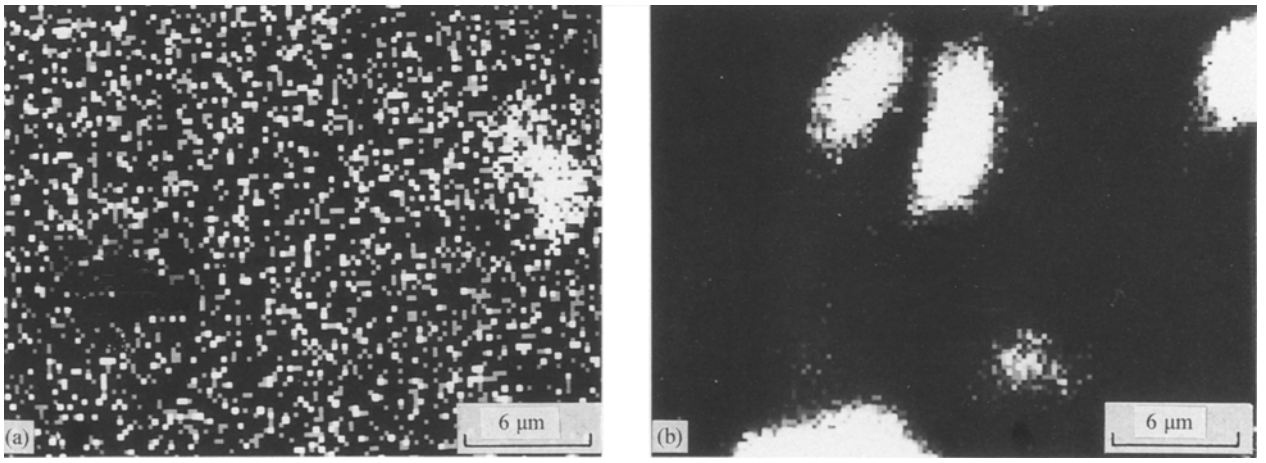

Figure 6 The X-ray maps (MgK_α) for the unreinforced alloy: (a) after 30 h at 175 °C, and (b) after 68 h at 175 °C.

around alumina particles was observed to increase with ageing time. Some segregation of Mg was also observed in the unreinforced alloy in the overaged condition after 18 h.

4. Discussion

The 6061 Al alloy precipitation sequence from the solid solution state may be described as follows: supersaturated metastable solid solution → GP zones (I and II) → rod shape metastable β′ → stable β (Mg_2Si) [13–15]. Precipitation from supersaturated solid solutions is started by the clustering of some solute atoms at some point in the matrix. These clusters – previously known as coherent clusters – consist mainly of silicon atoms [16]. These are generally known as GP zones and produce elastic strains,

due to different local lattice spacing as well as different local compositions, which increase the material resistivity. As the GP zones form, the hardness also increases due to the extra stress required to force dislocations through the coherent zones. With increasing ageing time more solute atoms diffuse into these clusters and make needle-shaped GP zones [17], which are called GP-II or the coherent β″-phase [16, 18]. As β″ increases more elastic strains are produced in the lattice, causing both the resistivity and hardness to increase. The elastic strains (which increase with the size of the precipitate) associated with the coherent interface raise the total energy of the system and it becomes energetically more favourable to replace the coherent precipitates with semi-coherent precipitates; therefore, the β′-phase is produced from the β″-phase, thus reducing the elastic strains. At this stage the resistivity starts to decrease while the hardness continues to increase. Further ageing coarsens the β′ phase and then the β-phase (Mg_2Si) that is nucleated from β′. The incoherent β-phase further reduces elastic energy in the lattice and thus decreases resistivity. The corresponding hardness values initially increase and then decrease (see Fig. 7).

The results of resistivity and hardness measurements show that addition of Al_2O_3 to 6061 aluminium alloy does not change the general precipitation sequence of the matrix. The resistivity measurements for the unreinforced and reinforced materials show three distinct stages. In stage I the resistivity is constant, an increase in resistivity occurs in stage II, and in stage III a decrease in resistivity with ageing time is observed (see Fig. 3). Stages I and II are longer for the unreinforced alloy. This means that the effect of the alumina particulates is to accelerate the kinetics of the ageing reaction. Comparing this effect to the ageing sequence in 6061 Al, stage I represents the time for nucleation of GP zones from the supersaturated solid solution. Since this time is shorter in the MMC than the unreinforced alloy, the incubation time in the MMC is smaller. Hardness results in the solution heat-treated state provide further evidence for a shorter nucleation time in the reinforced material (see Fig. 2). Stage II represents the formation of clusters, and the production and growth of GP zones. The shorter time to reach maximum hardness and resistivity in the MMC shows that the growth of precipitates is faster in this material. Nucleation and growth are diffusion controlled [19, 20]. Thus an acceleration of nucleation and growth is evidence of increased diffusion of solute atoms.

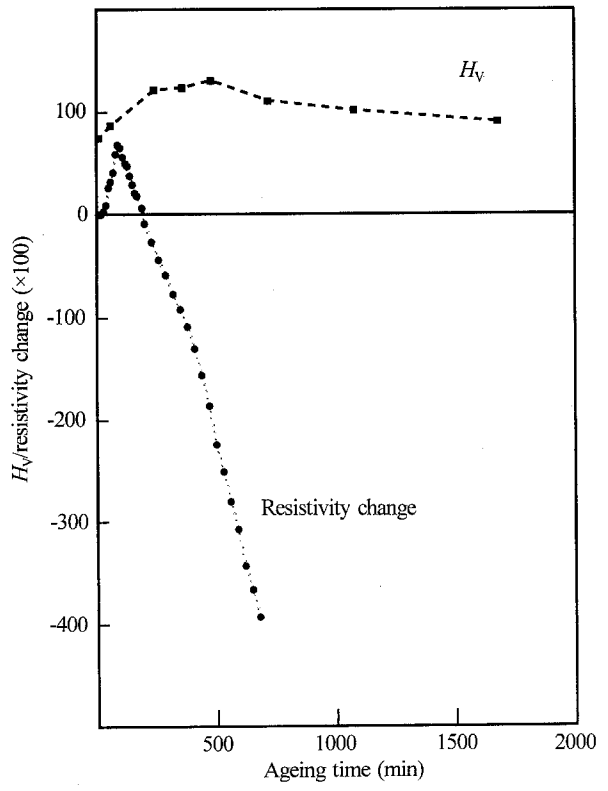

Figure 7 Comparison of: (■) H_V, and (●) resistivity change for the MMC.

Quenching to room temperature after solution treatment causes high-dislocation-density zones in MMCs [21, 22], and these zones form an easy path for the diffusion of atoms [12]. Since Mg has an atomic diameter of 0.32 nm compared to 0.24 nm for Si, the diffusion of Mg in Al is more difficult than that of Si in Al. Therefore diffusion of Mg controls the kinetics of the ageing reactions. The X-ray maps show the concentration of Mg to be nearly homogeneous in UA-unreinforced specimens, while some segregation is seen around reinforcing particles in the UA-MMC specimens. In addition, the degree of segregation increases with ageing time; therefore, this phenomenon shows an increase in the apparent diffusivity of magnesium by increasing the matrix dislocation density.

The much faster decrease of hardness in the MMC compared to the unreinforced alloy in the overaged condition can be explained by the higher diffusion rate of Mg in this material making larger β-precipitates which reduce the hardness. TEM micrographs from OA specimens (18 h at 175 °C) show small β′-precipitation in the unreinforced alloy but large precipitates in the reinforced alloy in the same overaged condition (Fig. 8). These particles are further evidence of accelerating ageing in the MMC.

The increase in resistivity can be used to identify the relative amount of GP zones. In the unreinforced alloy the resistivity rises more than in the reinforced material; and it would appear, therefore, that there was a greater volume fraction of GP zones in the unreinforced alloy. This is in agreement with the result of Papazian using a different technique [7]. As the amounts of Mg and Si in this material are constant, the smaller volume of GP zones in the MMC can be attributed to the fact that some Mg and Si elements have grown directly in the β′-phase.

5. Conclusions

1. The age-hardening sequences in microsphere-alumina-reinforced 6061 aluminium composite are similar to those of the unreinforced 6061 Al.

2. The microspherical particles considerably accelerate the precipitation hardening process aged at 175 °C by increasing the rate of both nucleation and growth of precipitation. Nucleation is accelerated by

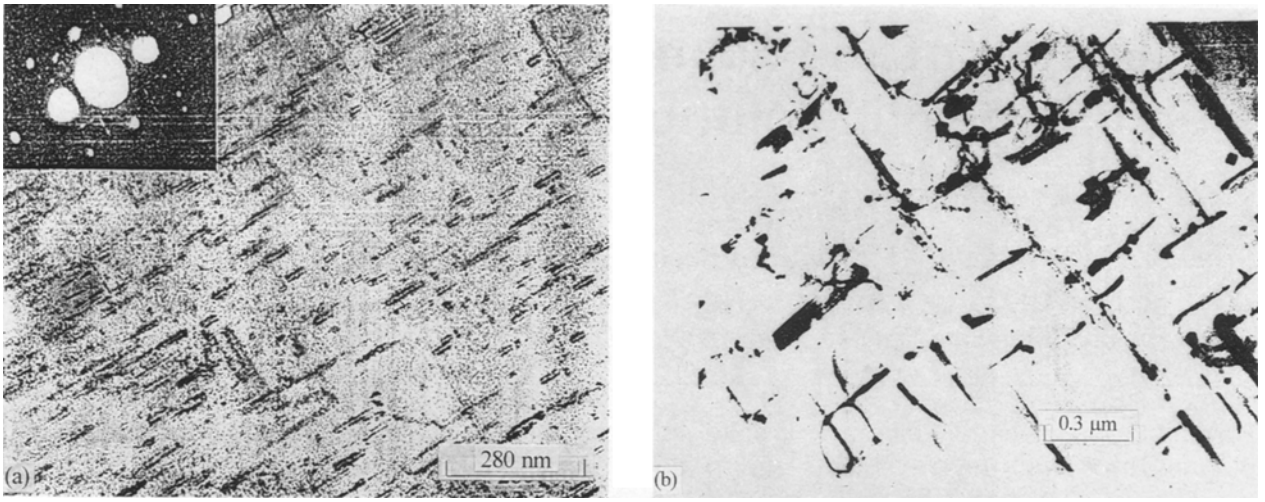

Figure 8 TEM micrographs of specimens after 18 h ageing at 175 °C: (a) β′-precipitates in the unreinforced alloy, and (b) β-precipitates (Mg_2Si) in the MMC.

the reinforcement particles due to the reduction of incubation time for coherent precipitates. The growth of precipitates is accelerated by increasing the solute diffusivity in the MMC.

3. The reinforcement addition is found to change the relative amounts of the various phases with a decrease in the volume fraction of the GP zones (GPI and II) but an increase in the production of β′ and β.

Acknowledgements

The authors wish to thank the Australian Research Council (ARC) Small Grants Scheme for the continuing support of this work. The materials were supplied for testing by Comalco Research Centre. M.J. Hadianfard is supported by a Junior Research Fellowship funded by the ARC.

References

1. H. J. RACK, in Proceedings of the Sixth International Conference on Composites, London, July 1987, Vol. 2, (Elsevier Applied Science, Amsterdam, 1987).
2. T. G. NIEH and R. F. KARLAK, *Scripta Metall.* **18** (1984) 27.
3. S. CERESERA and P. FIORINI, *Powder Metall.* **1** (1979) 1.
4. *Idem, ibid*, **4** (1981) 210.
5. R. D. SCHUELLER and F. E. WAWNER, *J. Mater. Sci.* **26** (1991) 3287.
6. C. M. FRIEND and S. D. LUXTON, *ibid.* **23** (1988) 3173.
7. J. M. PAPASIAN, *Metall. Trans. A* **19** (1988) 2945.
8. C. BADINI, F. MARINO and A. TOMASI, *Mater. Chem. Phys.* **25** (1990) 57.
9. M. VOGELSANG, R. J. ARSENAULT and R. FISHER, *Met. Trans A* **17** (1986) 379.
10. M. TAYA and T. MORI, *Acta Metall.* **35** (1987) 155.
11. R. J. ARSENAULT and R. M. FISHER, *Scripta. Metall.* **17** (1983) 67.
12. I. DUTTA and D. L. BOURELL, *Acta Metall. Mater.* **38** (1990) 2041.
13. C. ATONIONE, F. MARINO, G. RIONTINO, S. ABIS and E. DIRUSSO, *Mater. Chem. Phys.* **20** (1988) 13.
14. C. BADINI, F. MARINO and A. TOMASI, *J. Mater. Sci.* **26** (1991) 6279.
15. H. J. RACK and R. W. KRENZER, *Metall. Trans. A* **8** (1977) 335.
16. I. D. UTTA and S. M. ALLEN, *J. Mater. Sci. Lett.* **10** (1991) 323.
17. D. A. PORTER and K. E. EASTERLING, "Phase transformations in metals and alloys", (Van Nostrand Reinhold, Wokingham, England, 1981).
18. H. J. RACK and R. W. KRENZER, *Metall. Trans. A* **8** (1977) 335.
19. G. THOMAS, *J. Inst. Metals* **90** (1961–62) 57.
20. W. F. SMITH, "Structure and properties of engineering alloys", (McGraw-Hill, New York, 1981).
21. J. W. CAHN, *Acta Metall.* **5** (1957) 169.
22. E. P. BUTLER and P. SWANN, *Acta Metall.* **24** (1976) 343.

Received 22 October
and accepted 19 November 1992